JOURNAL OF NANO- AND ELECTRONIC PHYSICS *ЖУРНАЛ НАНО- ТА ЕЛЕКТРОННОЇ ФІЗИКИ*
Vol. **14** No 6, 06010(5pp) (2022) Том **14** № 6, 06010(5cc) (2022)

Squeezing MHD Flow along with Heat Transfer between Parallel plates by Using the Differential Transform Method

R. Agarwal

University of Petroleum and Energy Studies, 247001 Dehradun, India

(Received 15 October 2022; revised manuscript received 25 December 2022; published online 27 December 2022)

This research examines a squeezing flow with the characteristics of heat transfer in a viscous fluid. This fluid is squeezed between two parallel plates. The retrieved highly nonlinear equations are converted to a fourth-order single nonlinear differential equation for flow and a second-order differential equation for heat by using appropriate similarity transformation. A differential transform method (DTM) is applied to get the approximate solution of flow and heat transfer equations. The effect of different physical parameters is also discussed and presented graphically. To show the accuracy and exactness of DTM, numeric values of the skin-friction coefficient and Nusselt number are compared with previously published works and numerical methods.

Keywords: Squeezing flow, Differential transform method, Parallel plates, Magnetohydrodynamics (MHD), Heat transfer.

DOI: 10.21272/jnep.14(6).06010 PACS numbers: 44.05. + e, 47.65.Cb

1. INTRODUCTION

Because of many applications in different fields like edible industry, polymer processing, systems of lubrication, etc., squeezing flow is the most attractive research area among researchers. Squeezing flow plays a very powerful role in the field of chemical engineering. Stefan [1] investigated the basic theory of such a flow. Jackson [2] analyzed the squeeze flow of a liquid film between two parallel surfaces. Leider and Bird [3] and Singh et al. [4] discussed the same flow between parallel disks and plates, respectively. Hayat et al. [5] used nanofluid flow in their model. They also discussed the magnetic effect of making that fluid electrically conducting. Khan et al. [6] solved their model numerically by using the RKF4 method. Qayyum et al. [7] studied the asymmetric flow of a Jeffrey fluid. This fluid was compressed between two disks. They solved ODEs analytically by using HAM. Krishna and Chamkha [8] discussed such a flow in their model, where they used a nanofluid as a source fluid with water as a nanoparticle, which is compressed between two parallel disks. Srinivasacharya and Sreenath [9] deliberated a micropolar fluid flow squeezed between equidistant and stretchable plates.

Only some researchers obtained the exact solution because of the difficulty in solving the Navier-Stokes equation. So, to resolve this issue, the analytical solution is obtained by many mathematicians. DTM is a well-known method to get the solution of linear and nonlinear DEs. The basic theory of DTM is introduced by Zhou [10]. The base of this theory is the Taylor series. This method is developed on the electric circuit. DTM produced an analytical approximate solution in polynomial form. It has an iterative approach to get the approximate solution. Other analytical methods like HPM, HAM, and CM are also used to get the solution by many researchers. Hosseinzadeh et al. [11] investigated squeezing flow with the hydrothermal property of nanofluid, which is compressed between two plates, by using the HPM and collocation method. Mustafa et al. [12] employed HAM to solve non-dimensional ODEs of heat and mass transfer. Agarwal [13] studied the flow of a micropolar fluid between two disks, which has uniform permeability for suction by using HPM. Shirkhani et al. [14] performed flow characteristics of a Newtonian fluid. They solved numerically as well as analytically and got the perfect match between the results. To solve equations analytically, they used HPM, HAM, and CM while employing the fourth order Runge-Kutta method for its numerical solution. Agarwal and Mishra [15] used HPM for solving differential equations for their mathematical model. Sobamowo and Akinshilo [16] squeezed nanofluid between two parallel plates. They discussed the flow with the magnetic effect. They made nanofluid electrically conducting by inducing a magnetic field. Ahmad et al. [17] studied the Casson fluid flow and applied an analytical method to get the solution. Agarwal [18, 19] studied micropolar fluid and Reiner Rivlin fluid flow and used HPM to obtain its analytical solution.

In the current article, flow and transfer are discussed for an electrically viscous fluid. This fluid is compressed between two parallel plates. The obtained PDEs (nonlinear) are reconstructed into ODEs (nonlinear) by using similarity transformation. DTM is used to solve converted ODEs. The impact of the squeeze parameter, magnetic field, Prandtl, and Eckert number is discussed and shown in pictorial form. The coefficient of skin friction and Nusselt number are tabulated and compared with the literature to validate the results of DTM.

2. MATHEMATICAL FORMULATION

Let us contemplate an incompressible and unsteady flow of a viscous fluid between two infinite parallel plates. Both the plates are at a distance D apart, where $D = \pm s(t) = \pm \ell(1-\alpha t)^{1/2}$ and ℓ is the distance between plates at a time $t = 0$. Here, α represents a squeeze parameter and it is inversely proportional to time t, i.e., $\alpha \propto \frac{1}{t}$. When $\alpha > 0$, it means both plates are compressed to each other, and $\alpha < 0$ shows that both plates are going away from each other. The effect of the viscous dissipation function is maintained in the model as heat generation at the moment of friction, which is produced by shear in the flow. Since the source fluid is extremely viscous and its speed is too high, then high Eckert number ($\gg 1$) is considered to visualize the importance of the viscous dissipation function. A constant magnetic field of the strength M_n is induced vertically on plates. No other electric field acting on the plates is assumed.

The governing equations are

$$\frac{\partial u_x}{\partial x}+\frac{\partial v_y}{\partial y}=0, \quad (1)$$

$$\frac{\partial u_x}{\partial t}+u_x\frac{\partial u_x}{\partial x}+v_y\frac{\partial u_x}{\partial y}=-\frac{1}{\rho}\frac{\partial P}{\partial x}+\gamma\left(\frac{\partial^2 u_x}{\partial x^2}+\frac{\partial^2 u_x}{\partial y^2}\right)-\frac{\sigma {B_0}^2 u_x}{\rho}, \quad (2)$$

$$\frac{\partial v_y}{\partial t}+u_x\frac{\partial v_y}{\partial x}+v_y\frac{\partial v_y}{\partial y}=-\frac{1}{\rho}\frac{\partial P}{\partial y}+\gamma\left(\frac{\partial^2 v_y}{\partial x^2}+\frac{\partial^2 v_y}{\partial y^2}\right), \quad (3)$$

$$\frac{\partial T}{\partial t}+u_x\frac{\partial t}{\partial x}+v_y\frac{\partial T}{\partial y}=\frac{\kappa}{\rho c_p}\left(\frac{\partial^2 T}{\partial x^2}+\frac{\partial^2 T}{\partial y^2}\right)+\frac{\gamma}{c_p}\left[4\left(\frac{\partial u_x}{\partial x}\right)^2+\left(\frac{\partial u_x}{\partial y}+\frac{\partial v_y}{\partial x}\right)^2\right]. \quad (4)$$

Here, velocities along the x and y axes are taken as u_x and v_y, T and P denote the temperature and pressure, respectively, ρ is the density of the fluid, κ is the thermal conductivity, γ is the kinematic viscosity, c_p denotes the specific heat, B_0 is the magnitude of the induced magnetic field.

The problem is supported by the following conditions:

$$u_x=0,\ v_y=v_\omega=\frac{ds}{dt},\quad T=T_S,\ \text{at } y=s(t),$$
$$\frac{\partial u_x}{\partial y}=0,\ v_y=0,\quad \frac{\partial T}{\partial y}=0,\ \text{at } y=0. \quad (5)$$

Wang [20] introduced transformation for 2D flow, which is as follows:

$$u_x=\frac{\alpha x}{2(1-\alpha t)}F'(\xi),\qquad v_y=-\frac{\alpha \ell}{2(1-\alpha t)^{1/2}}F(\xi). \quad (6)$$

Here, $\xi=\frac{y}{\ell(1-\alpha t)^{1/2}}$ is a dimensionless parameter. Using the transformation given in Eq. (6), we rewrite Eqs. (2)-(4), by eliminating the term of pressure and get the following:

$$F^{iv}-S_q(\xi F'''+3F''+F'F''-FF''')-{M_n}^2F''=0, \quad (7)$$

$$\theta''+P_rS_q(F\theta'-\xi\theta')+P_rE_c\left({F''}^2+4\epsilon^2{F'}^2\right)=0 \quad (8)$$

with modified conditions at the boundary

$$F(0)=0,\quad F''(0)=0,\quad \theta'(0)=0,$$
$$F(1)=1,\quad F'(1)=0,\quad \theta(1)=0, \quad (9)$$

where $S_q\left[=\frac{\alpha\ell^2}{2\gamma}\right]$ is the squeeze parameter with the property $S_q>0$ when plates are going away and $S_q<0$ when plates are coming closer to each other. $P_r\left[=\frac{\mu c_p}{\kappa}\right]$ is the Prandtl number and $E_c\left[=\frac{1}{c_p}\left(\frac{\alpha x}{2(1-\alpha t)}\right)^2\right]$ is the Eckert number. ${M_n}^2\left[=\frac{\sigma\ell^2}{\rho\gamma}{B_0}^2\right]$ is the magnetic parameter and $\epsilon\left[=\frac{\ell}{x}\right]$ is a dimensionless parameter. It must be noted that the Eckert number equals to zero in the absence of the viscous dissipation effect.

The skin-friction coefficient is defined by

$$C_{sf}=\frac{\mu\left(\frac{\partial u_x}{\partial y}\right)_{y=h(t)}}{\rho {v_\omega}^2},$$

its non-dimensional form is

$$(1-\alpha t)\frac{x^2}{\ell^2}R_{oL}C_{sf}=F''(1). \quad (10)$$

Here, $R_{oL}\left[=\frac{\alpha\ell^5\rho}{2\mu x^3\sqrt{(1-\alpha t)}}\right]$ is the local Reynolds number.

The Nusselt number is $N_u=-\frac{\ell\left(\frac{\partial T}{\partial y}\right)_{y=h(t)}}{T_S}$, its non-dimensional form is

$$\sqrt{(1-\alpha t)}N_u=-\theta'(1). \quad (11)$$

3. METHODOLOGY OF DTM

k times differentiation of $f(x)$ in this method is given by

$$F(k)=\frac{1}{k!}\left(\frac{d^kf(x)}{dx^k}\right)_{x=x_0}. \quad (12)$$

The inverse transformation of $F(k)$ is defined by

$$f(x)=\sum_{k=0}^{\infty}F(k)\,(x-x_0)^k. \quad (13)$$

$f(x)$ can be shown in the form of finite series and hence Eq. (13) can be expressed as

$$f(x)=\sum_{k=0}^{n}F(k)\,(x-x_0)^k. \quad (14)$$

From Eq. (12) and Eq. (13), we get

$$f(x)=\sum_{k=0}^{\infty}(x-x_0)^k\frac{1}{k!}\left(\frac{d^kf(x)}{dx^k}\right)_{x=x_0},$$

which represents the Taylor series form of $f(x)$ at $x=x_0$. The following theorems T_i ($i\le 10$) can be concluded from Eq. (12) and Eq. (13):

T_1: If $f(x)=g(x)\pm h(x)$, then $F(k)=G(k)\pm H(k)$.
T_2: If $f(x)=cg(x)$, then $F(k)=cG(k)$, where c is a constant.
T_3: If $f(x)=\frac{d^mg(x)}{dx^m}$, then $F(k)=\frac{(k+m)!}{k!}G(k+m)$.
T_4: If $f(x)=g(x)h(x)$, then $F(k)=\sum_{k_1=0}^{k}G(k_1)H(k-k_1)$.
T_5: If $f(x)=e^{ix}$, then $F(k)=\frac{x^k}{k!}$.
T_6: If $f(x)=x^n$, then $F(k)=\delta(k-n)$, where $\delta(k-n)=\begin{cases}1, & k=n\\ 0, & k\neq n\end{cases}$
T_7: If $f(x)=g_1(x)g_2(x)\ldots\ldots\ldots.g_n(x)$, then $F(k)=\sum_{k_{n-1}=0}^{k}\sum_{k_{n-2}=0}^{k_{n-1}}\sum_{k_1=0}^{k_2}G_1(k_1)G_2(k_2-k_1)\ldots G_n(k-k_{n-1})$.
T_8: If $f(t)=(1+t)^m$, then $F(k)=\frac{m(m-1)\ldots\ldots\ldots(m-k+1)}{k!}$.
T_9: If $f(t)=\sin(\omega t+\alpha)$, then $F(k)=\frac{\omega^k}{k!}\sin\left(\frac{\pi k}{2}+\alpha\right)$.
T_{10}: If $f(t)=\cos(\omega t+\alpha)$, then $F(k)=\frac{\omega^k}{k!}\cos\left(\frac{\pi k}{2}+\alpha\right)$.

4. APPLICATION OF DTM

Initially, we will transform Eq. (7) and Eq. (8) under the above-mentioned theorems. Then we get the following iterative equations:

$$(\lambda+4)(\lambda+3)(\lambda+2)(\lambda+1)F(\lambda+4) - S_q\big[(\lambda+2)(\lambda+1)\lambda F(\lambda+2) + 3(\lambda+2)(\lambda+1)F(\lambda+2) + \sum_{n=0}^{\lambda}(n+1)F(n+1)(\lambda-n+2)(\lambda-n+1)F(\lambda-n+3)\big] - {M_n}^2(\lambda+2)(\lambda+1)F(\lambda+2) = 0, \quad (15)$$

$$(\lambda+2)(\lambda+1)\theta(\lambda+2) + P_r S_q\big[\sum_{n=0}^{\lambda} F(n)(\lambda-n+1)\,\theta(\lambda-n+1) - \lambda\theta(n)\big] + P_r E_c\big[\sum_{n=0}^{\lambda}(n+2)(n+1)F(n+2)(\lambda-n+2)\,(\lambda-n+1)F(\lambda-n+2) \quad + 4\epsilon^2\sum_{n=0}^{\lambda}(n+1)F(n+1)(\lambda-n+1)F(\lambda-n+1)\big] = 0 \quad (16)$$

with the following transformed boundary conditions:

$$F(0)=0, \quad F(1)=a, \quad F(2)=0,$$
$$F(3)=b, \quad \theta(0)=c, \quad \theta(1)=0,$$

where a, b, c are evaluated by applying appropriate conditions mentioned in Eq. (9). We will get the approximate solution of $F(\xi)$ and $\theta(\xi)$ by using iteration from Eq. (15) and Eq. (16).

5. RESULTS AND DISCUSSION

In this segment, the author highlights the impact of various parameters on the radial velocity $F'(\xi)$, axial velocity $F(\xi)$, and temperature profile $\theta(\xi)$. For the validation of the DTM, the author presented comparative data of the outcomes calculated by DTM with the outcomes evaluated by the numerical method, as well as results available in previous studies. This comparison is tabulated in Table 1 and Table 2.

The impact of M_n on both profiles is pictured in Fig. 1-Fig. 3 by keeping other parameters fixed $S_q = P_r = E_c = 1, \epsilon = 0.1$. Fig. 1 defines the behavior of $F'(\xi)$ for distinct values of M_n. This graph tells that velocity declines with rising in M_n up to the middle of the entire gap length while escalating with a rise in M_n. The effect of M_n on the axial velocity is shown in Fig. 2, which describes the continuous increment in the velocity from the lower boundary to the upper boundary. A decrement in the velocity profile with rising the magnitude of M_n can also be observed from this figure. The profile of temperature for the various numeric values of the magnetic parameter is graphed in Fig. 3. This figure elucidates that temperature gets down by increasing the values of the parameter while near the upper plate; its behavior is not significant.

The effect of the squeeze parameter (S_q) is discussed in Fig. 4-Fig. 9. Two cases of the squeeze parameter are presented here, when S_q is positive, i.e., both the plates are moving away and when S_q is negative, i.e., both plates are moving toward to each other. The first case, when $S_q > 0$, is pictured in Fig. 7-Fig. 9 by taking $M_n = P_r = E_c = 1, \epsilon = 0.1$. The nature of the radial velocity for the distinct values of the squeeze parameter is shown in Fig. 4 and Fig. 7. In both figures, the nature of the flow is similar. These figures interpret that velocity goes down near the lower plate and it goes up near the upper plate after increasing the gap between both the plates. Fig. 5 and Fig. 8 illustrate the nature of the axial velocity for both above-mentioned cases. In both graphs, velocity increases rapidly in the entire gap length from the lower to the upper boundary. One more observation that velocity falls with increasing magnitude of the squeeze parameter can also be observed. From Fig. 6 and Fig. 9, it can be noted that the squeeze parameter and temperature are inversely proportional to each other. In other words, the temperature reduces by increasing the magnitude of the squeeze parameter. Fig. 10 explains that temperature escalates with the rise in the values of the Prandtl number under the fact that temperature ∝ Prandtl number. According to Fig. 11, on rising the values of the Eckert number, the temperature gets up.

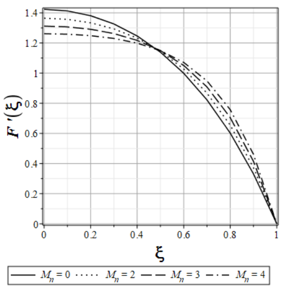

Fig. 1 – Influence of M_n

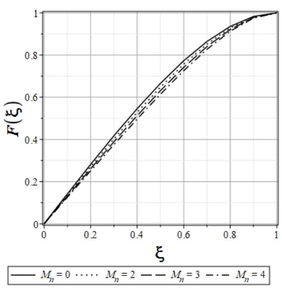

Fig. 2 – Influence of M_n

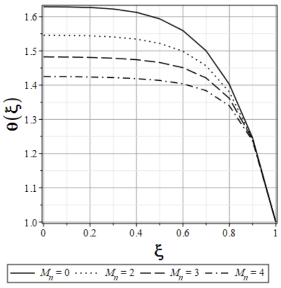

Fig. 3 – Influence of M_n

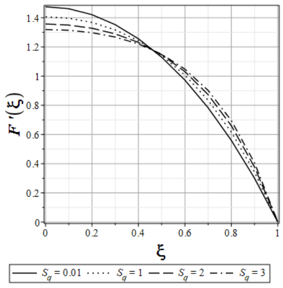

Fig. 4 – Influence of $S_q(>0)$

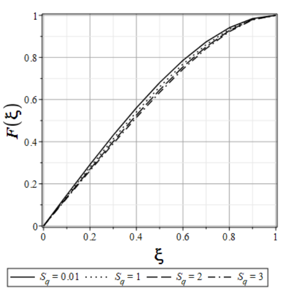

Fig. 5 – Influence of $S_q(>0)$

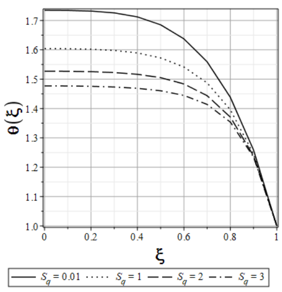

Fig. 6 – Influence of $S_q(>0)$

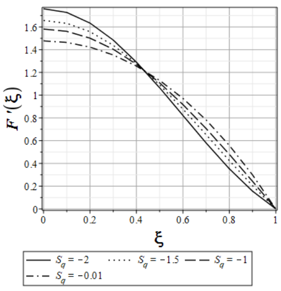

Fig. 7 – Influence of $S_q(<0)$

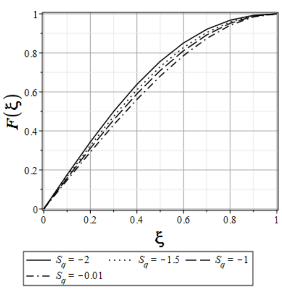

Fig. 8 – Influence of $S_q(<0)$

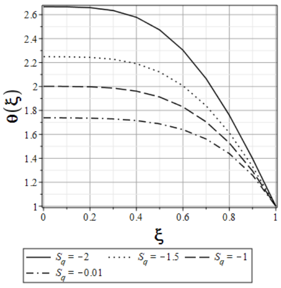

Fig. 9 – Influence of $S_q (< 0)$

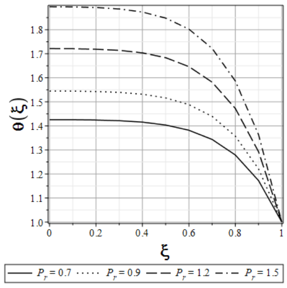

Fig. 10 – Influence of P_r

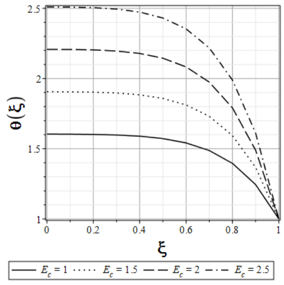

Fig. 11 – Influence of E_c on temperature

Table 1 – Comparative data of the coefficient of skin-friction and Nusselt number when $M_n = 0, P_r = E_c = 1, \epsilon = 0.1$

S_q	$-F''(1)$		$-\theta'(1)$	
	[12]	Present	[12]	Present
– 1	2.170090	2.170067	3.319899	3.318904
– 0.5	2.614038	2.617401	3.129491	3.129454
0.01	3.007134	3.007134	3.047092	3.047092
0.5	3.336449	3.336453	3.026324	3.026259
2	4.167389	4.167643	3.118551	3.109581

Table 2 – Comparative data of the coefficient of skin-friction and Nusselt number when $M_n = 1, P_r = E_c = 1, \epsilon = 0.1$

S_q	$-F''(1)$		$-\theta'(1)$	
	DTM	NM	DTM	NM
– 1	2.424458	2.424488	3.235517	3.236036
– 0.5	2.836849	2.836852	3.103296	3.103284
0.01	3.201236	3.201236	3.052358	3.052359
0.5	3.512310	3.512305	3.048463	3.048652
1	3.799759	3.799720	3.070164	3.071676

6. CONCLUSIONS

Squeezing flow in an electrically conducting viscous fluid and attributes of the temperature are examined between two equidistant plates. Nonlinear ODEs for flow and temperature profiles are achieved by using appropriate transformations. DTM is applied to get the analytical solution. A comparative data of the coefficient of skin friction and the Nusselt number in the absence of the magnetic field with literature is tabulated, which validates the accuracy and validity of DTM. The value in the existence of a magnetic field is compared with the results evaluated by the numerical method. The influence of various parameters is displayed by graphs along with a detailed discussion.

REFERENCES

1. J. Stefan, *Annalen der Physik* **230**, 316 (1875).
2. J.D. Jackson, *Appl. Sci. Res., Section A* **11**, 148 (1963).
3. P.J. Leider, R.B. Bird, *Industrial Eng. Chem. Fundamentals* **13**, 336 (1974).
4. P. Singh, V. Radhakrishnan, K.A. Narayan, *Ingenieur-Archiv* **60**, 274 (1990).
5. T. Hayat, T. Muhammad, A. Qayyum, A. Alsaedi, M. Mustafa, *J. Molec. Liquid.* **213**, 179 (2016).
6. U. Khan, N. Ahmed, S.T. Mohyud-Din, *Appl. Thermal Eng.* **113**, 1107 (2017).
7. A. Qayyum, M. Awais, A. Alsaedi, T. Hayat, *Chin. Phys. Lett.* **29**, 034701 (2012).
8. M.V. Krishna, A.J. Chamkha, *J. Porous Media* **22**, 209 (2019).
9. D. Srinivasacharya, I. Sreenath, *Heat Transfer – Asian Research* **48**, 2155 (2019).
10. J.K. Zhou, *Huazhong University Press, Wuhan, China*, (1986).
11. K. Hosseinzadeh, M. Alizadeh, D.D. Ganji, *Int. J. Mechan. Mater. Eng.* **13**, 1 (2018).
12. M. Mustafa, T. Hayat, S. Obaidat, *Meccanica* **47** No 7, 1581 (2012).
13. R. Agarwal, *PalArch's Journal of Archaeology of Egypt/ Egyptology* **17**, 903 (2020).
14. M.R. Shirkhani, H.A. Hoshyar, I. Rahimipetroudi, H. Akhavan, D.D. Ganji, *Propulsion and Power Research* **7**, 247 (2018).
15. R. Agarwal, P.K. Mishra, *Mater. Today: Proc.* **46**, 10153 (2021).
16. M.G. Sobamowo, A.T. Akinshilo, *Alexandria Eng. J.* **57**, 1413 (2018).
17. N. Ahmed, U. Khan, S.I. Khan, S. Bano, S.T. Mohyud-Din, *J. King Saud University-Science* **29**, 119 (2017).
18. R. Agarwal, *Mater. Today: Proc.* **46**, 10227 (2021).
19. R. Agarwal, *Palestine Journal of Mathematics* **11**, 184 (2022).
20. C.Y. Wang, *J. Appl. Mechanics* **43**, 579 (1976).

Стиснення MHD потоку разом із теплопередачею між паралельними пластинами за допомогою методу диференціального перетворення

R. Agarwal

University of Petroleum and Energy Studies, Dehradun 247001, India

У дослідженні вивчається стискаючий потік із характеристиками теплопередачі у в’язкій рідині. Ця рідина затиснута між двома паралельними пластинами. Отримані сильно нелінійні рівняння перетворюються на єдине нелінійне диференціальне рівняння четвертого порядку для потоку та диференціальне рівняння другого порядку для тепла за допомогою відповідного перетворення подібності. Для отримання наближеного розв’язку рівнянь потоку та теплопередачі застосовано метод диференціального перетворення (DTM). Вплив різних фізичних параметрів також обговорюється та представлено графічно. Щоб показати точність і безпомилковість DTM, числові значення коефіцієнта поверхневого тертя та числа Нуссельта порівнюються з результатами раніше опублікованих робіт та чисельних методів.

Ключові слова: Стискаючий потік, Метод диференціального перетворення, Паралельні пластини, Магнітогідродинаміка (MHD), Теплообмін.